Published in final edited form as:
J Immunol. 2011 August 15; 187(4): 1970–1976. doi:10.4049/jimmunol.1100841.

HIF-2α regulates GM-CSF-derived sVEGFR-1 production from macrophages and inhibits tumor growth and angiogenesis[1]

Julie M. Roda[*], **Laura A. Sumner**[*], **Randall Evans**[*], **Gary S. Phillips**[†], **Clay B. Marsh**[*], and **Timothy D. Eubank**[*,‡]

[*]The Dorothy M. Davis Heart and Lung Research Institute, Division of Pulmonary, Allergy, Critical Care, and Sleep Medicine, Department of Internal Medicine, The Ohio State University College of Medicine, Columbus, OH 43210, USA

[†]The Center for Biostatistics, The Ohio State University College of Medicine, Columbus, OH 43210, USA

[‡]The Comprehensive Cancer Center, The Ohio State University College of Medicine, Columbus, OH 43210, USA

Abstract

Macrophage secretion of VEGF in response to the hypoxic tumor microenvironment contributes to tumor growth, angiogenesis, and metastasis. We have recently demonstrated that macrophages stimulated with GM-CSF at low O_2 secrete high levels of a soluble form of the VEGF receptor (sVEGFR-1), which neutralizes VEGF and inhibits its biological activity. Using siRNA targeting to deplete HIF-1α or HIF-2α in murine macrophages, we found that macrophage production of sVEGFR-1 in response to low O_2 was dependent on HIF-2α, while HIF-1α specifically regulated VEGF production. In our current report, we evaluated the growth of B16F10 malignant melanoma in mice with a monocyte/macrophage-selective deletion of HIF-1α or HIF-2α (HIF-1α$^{flox/flox}$-or HIF-2α$^{flox/+}$/LysMcre mice). GM-CSF treatment increased intra-tumoral VEGF and sVEGFR-1 in control mice, an effect that was associated with a decrease in microvessel density. GM-CSF treatment of HIF-1α$^{flox/flox}$/LysMcre mice induced sVEGFR-1 but not VEGF, resulting in an overall greater reduction in tumor growth and angiogenesis compared to control mice. In addition, real-time PCR for melanoma-specific genes revealed a significantly reduced presence of lung micrometastases in HIF-1α$^{flox/flox}$/LysMcre mice treated with GM-CSF. Conversely, GM-CSF treatment induced VEGF but not sVEGFR-1 in HIF-2α$^{flox/+}$/LysMcre mice, and correspondingly, GM-CSF did not decrease tumor growth, angiogenesis, or lung metastasis in these mice. This study reveals opposing roles for the HIFs in the regulation of angiogenesis by tumor-associated macrophages, and suggests that administration of GM-CSF might be an effective means of inducing sVEGFR-1 and inhibiting tumor growth and angiogenesis in patients with melanoma.

INTRODUCTION

An abundance of tumor-associated macrophages is associated with poor clinical outcome in numerous human cancers, including breast, ovarian, and prostate cancer (1–3). Tumor-associated macrophages contribute to tumor progression, in part, through their section of the potent angiogenic molecule vascular endothelial growth factor (VEGF), which is driven largely by the low O_2 concentration within the tumor microenvironment (4, 5). In addition to

[1]This study was supported by NCI K99 CA131552-01 (T.D.E), NIH T32 HL07946-06 (J.R.), and R01 HL067167 (C.B.M.).

Contact Tim D. Eubank, PhD, tim.eubank@osumc.edu, Phone: 614-292-9958, Fax: 614-688-4662, Clay B. Marsh, MD, Clay.marsh@osumc.edu, Phone: 614-293-9309, Fax: 614-688-4662.

VEGF, hypoxia upregulates the expression of the VEGF receptor (VEGFR-1), as well as genes involved in anaerobic metabolism, cell survival, and proliferation (6). In addition to the membrane-bound isoform of VEGFR-1, macrophages secrete a soluble form of the VEGF receptor (sVEGFR-1) (7), which results from alternative splicing of the same gene transcript (8). sVEGFR-1 comprises the extracellular ligand-binding domain of the membrane-bound form of the receptor, and serves as a potent antagonist of VEGF signaling by sequestering VEGF and inhibiting its interaction with the transmembrane receptors (9). Based on the observation that both VEGF and the VEGF receptor contain a hypoxia-responsive promoter element, we previously examined the effect of hypoxia on GM-CSF-induced sVEGFR-1 production. We found that in addition to VEGF, macrophages stimulated with GM-CSF secreted high levels of sVEGFR-1, which bound and neutralized the VEGF. Furthermore, sVEGFR-1 secretion from GM-CSF-stimulated macrophages increased with decreasing O_2 concentration (10). These findings suggested that hypoxia, canonically thought to promote angiogenesis, could induce the secretion of anti-angiogenic molecules within a GM-CSF-rich environment.

The transcriptional response to hypoxia is driven primarily by a family of transcription factors known as the hypoxia inducible factors (HIFs). The HIFs are constitutively transcribed but are rapidly degraded under normoxic conditions, principally through the hydroxylation of proline residues by prolyl hydroxylase domain (PHD) proteins, of which there are three isoforms (PHD1-3). This modification allows binding of the von Hippel-Lindau (VHL) E3 ubiquitin ligase, which targets the HIF for ubiquitination and proteasomal degradation. Hypoxia promotes HIF protein accumulation by inhibiting PHD-mediated proline hydroxylation, as O_2 is the rate-limiting co-factor in the hydroxylation reaction. The exact contribution of HIF-1α and HIF-2α to the regulation of hypoxic gene expression appears to vary between cell types, although a number of studies suggest that HIF-2α is primarily upregulated by hypoxic macrophages (11, 12). In order to determine which of the HIFs was responsible for sVEGFR-1 production in hypoxic macrophages, we utilized macrophages from mice deficient in HIF-1α or HIF-2α in the monocyte/macrophage lineage (HIF-1α$^{flox/flox}$- or HIF-2α$^{flox/+}$/LysMcre mice). HIF-1α-deficient macrophages cultured with GM-CSF at 0.5% O_2 produced less VEGF than control macrophages under the same conditions, while sVEGFR-1 secretion was unaffected. In contrast, deletion of HIF-2α inhibited the production of sVEGFR-1 in response to GM-CSF and low O_2, without affecting VEGF production (10). These findings suggested that HIF-1α drives macrophage production of VEGF in response to GM-CSF and low O_2, while HIF-2α controls sVEGFR-1 production.

In the current report, we examined melanoma growth and response to GM-CSF therapy in mice with HIF-1α- or HIF-2α-deficient tumor macrophages. GM-CSF treatment of control mice induced a low amount of VEGF production and a much greater production of sVEGFR-1, resulting in a net decrease in tumor growth and angiogenesis. Deletion of HIF-1α from tumor-associated macrophages inhibited VEGF production in response to GM-CSF with no effect on sVEGFR-1 production, resulting in an even greater reduction in tumor growth and angiogenesis than was observed in GM-CSF-treated control mice. Conversely, deletion of HIF-2α from tumor-associated macrophages inhibited sVEGFR-1 production in response to GM-CSF with no effect on VEGF production and abrogated the anti-tumor response to GM-CSF.

MATERIALS AND METHODS

Generation of HIF-1α$^{flox/flox}$/LysMcre and HIF-2α$^{flox/+}$/LysMcre mice

HIF-1α$^{flox/flox}$/LysMcre were originally developed by Dr. Randall Johnson, University of California at San Diego, and were obtained from Dr. Philip Popovich of The Ohio State

University. These mice were generated by crossing a C57BL/6 mouse containing *loxP* sequences flanking the *HIF1A* gene with a C57BL/6 mouse expressing Cre recombinase from the lysozyme M (LysM) promoter, which is expressed only in myeloid lineage cells (13). HIF-2$\alpha^{flox/flox}$ mice (originally developed by Dr. Celeste Simon, University of Pennsylvania (14)) and LysMcre recombinase mice (originally developed by Irmgard Foerster, University of Duesseldorf (15)) (both purchased from The Jackson Laboratory, Bar Harbor, ME) were crossed to generate mice heterozygous for both LysMcre and the floxed HIF-2α allele. These mice were then bred with each other, and HIF-2$\alpha^{flox/+}$/LysMcre offspring, which are heterozygous for the floxed HIF-2α allele and homozygous for LysM-driven cre recombinase, were selected for use in these studies. C57BL/6 mice expressing LysMcre recombinase but no floxed alleles were used as controls.

Murine melanoma tumor model

6–8-week-old HIF-1$\alpha^{flox/flox}$/LysMcre mice, HIF-2$\alpha^{flox/+}$/LysMcre mice, or LysMcre control mice were injected with 1×10^5 B16F10 murine melanoma cells subcutaneously on the left flank. Once tumors become palpable (approximately 5 days), mice were randomly allocated to receive treatment with either PBS (negative control) or with murine GM-CSF (100 ng per mouse in a 50μL volume). Mice were treated intratumorally 3 times per week until tumors reached a size of 20 mm in any dimension (approximately 2.5 weeks), at which point mice were euthanized, in accordance with institutional policy. Tumor diameters were measured 3 times per week with calipers, and tumor volumes were calculated as follows: Tumor volume = $0.5 \times [(\text{large diameter}) \times (\text{small diameter})^2]$. For experiments analyzing the effect of neutralizing sVEGFR-1 in combination with GM-CSF treatment, mice were treated intratumorally 3×/week with either PBS or GM-CSF and 4 μg anti-VEGFR-1 neutralizing antibody (R&D Systems) or 4 μg polyclonal goat IgG isotype control (Santa Cruz Biotechnology). All protocols were approved by the Ohio State University Animal Care and Use Committee, and mice were treated in accordance with institutional guidelines for animal care.

Texas red-dextran staining for tumor angiogenesis

HIF-1$\alpha^{flox/flox}$/LysMcre mice, HIF-2$\alpha^{flox/+}$/LysMcre mice, or LysMcre control mice were inoculated with B16F10 melanomas and treated 3×/week with intratumoral PBS or GM-CSF, as described above. Five minutes prior to sacrifice, mice were administered Texas red-conjugated dextran (molecular weight 70,000, Invitrogen/Molecular Probes) via tail vein injection (20 μg dextran/g of mouse weight) and subsequently perfused for 5 minutes with PBS. Tumor sections were visualized by fluorescent microscopy and analyzed blindly. Functional blood vessels (Texas red-positive) were identified and quantified using Adobe Photoshop CS2 histogram analysis.

Real-time PCR

Organs collected from mice at the time of euthanasia were flash-frozen in liquid nitrogen, pulverized, and dissolved in Trizol reagent (Invitrogen). RNA was extracted in chloroform and then purified using the RNeasy Minikit (Qiagen). cDNA was generated from 1 μg of RNA using the Superscript First Strand Synthesis System (Invitrogen) and used for real-time PCR using SYBR Green PCR Master Mix (Applied Biosciences). Primer sets were designed using Primer Express v3.0 software (ABI Prism, Perkin-Elmer) and synthesized by Invitrogen, and have been described previously (10). Data were analyzed according to the comparative threshold method and normalized against the GAPDH internal control transcript. Results are semi-quantitative and represent the relative expression of a transcript in a particular treatment group as compared with levels in PBS-treated control mice.

Evaluation of lung metastases

Lung metastases were evaluated by detection of mRNA for melanocyte-specific proteins within the lungs of tumor-bearing mice. B16F10 tumor-bearing HIF-1α$^{flox/flox}$/LysMcre mice, HIF-2α$^{flox/+}$/LysMcre mice, or LysMcre control mice were treated with intratumoral PBS or GM-CSF, as described above. At the time of sacrifice, lungs were excised and flash-frozen in liquid nitrogen. RNA was extracted and cDNA was generated as described above. The melanocyte-specific mRNAs TRP2 and Pmel17 were detected by nested PCR using a modification of the protocol described by Tsukamoto *et al*. (16). For the initial reaction, 30 cycles of PCR were carried out (95°C for 1 minute, 58°C for 1 min, 72°C for 1 min) in a 20 μl reaction volume containing 2 μl of cDNA. For reamplification with the nested primers, 1 μL of the first reaction product was amplified in a 20 μl reaction volume for a further 30 cycles. Data were analyzed according to the comparative threshold method and normalized against the GAPDH internal control transcript. Results are semi-quantitative and represent the fold difference in transcript levels in HIF-1α$^{flox/flox}$- or HIF-2α$^{flox/+}$/LysMcre mice as compared with levels in PBS-treated LysMcre control mice.

Statistical analyses

The ANOVA test was used to compare independent measurements between multiple treatment groups. The data was log-transformed to normalize the variance across groups. P-values were adjusted using the Holm's procedure to conserve the type I error at 0.05 due to the multiple comparisons. For tumor growth data, changes in tumor volume over time were assessed via a longitudinal model. Tumor values were log-transformed, and estimated slopes (changes in tumor volume over time) were calculated with 95% confidence intervals. Estimated differences in tumor volume were calculated by a random-effects regression of the longitudinal data. For all analyses, $p \leq 0.05$ was considered statistically significant.

RESULTS

Growth of B16F10 melanomas is inhibited in mice with HIF-1α-deficient macrophages

Our previous studies showed that deletion of HIF-1α inhibits macrophage production of VEGF in response to GM-CSF and low O_2, with no effect on sVEGFR-1 production under the same conditions, *in vitro* (10). We therefore hypothesized that tumor growth would be decreased in HIF-1α$^{flox/flox}$/LysMcre mice, due to a decrease in VEGF production from HIF-1α-deficient tumor-infiltrating macrophages. HIF-1α$^{flox/flox}$/LysMcre mice or LysMcre control mice were inoculated with B16F10 tumors and treated with intratumoral PBS or GM-CSF. As shown in Figure 1A, tumor growth was decreased in HIF-1α$^{flox/flox}$/LysMcre mice as compared to LysMcre control mice, even in the absence of GM-CSF therapy (p = 0.002). Furthermore, GM-CSF treatment of HIF-1α$^{flox/flox}$/LysMcre mice further decreased tumor growth compared to GM-CSF-treated control mice. These results demonstrated that the selective deletion of HIF-1α from tumor-infiltrating macrophages could decrease tumor growth and increase the anti-tumor effects of GM-CSF.

GM-CSF does not inhibit tumor growth in mice with HIF-2α-deficient macrophages

We next examined the effect of HIF-2α deletion on melanoma growth. In our previous studies, deletion of HIF-2α inhibited macrophage production of sVEGFR-1 in response to GM-CSF, with no effect on VEGF production (10). We therefore hypothesized that tumor growth would not be reduced by GM-CSF in HIF-2α$^{flox/+}$/LysMcre mice, due to the inability of tumor-infiltrating macrophages to secrete sVEGFR-1 in these mice. As previously observed, treatment of LysMcre control mice with GM-CSF significantly inhibited tumor growth (p = 0.019). However, GM-CSF had no effect on tumor growth in HIF-2α$^{flox/+}$/LysMcre mice (p = 0.318) (Figure 1B). These results suggest that HIF-2α

expression in tumor-infiltrating macrophages contributes to the anti-tumor effects of GM-CSF, possibly through the secretion of sVEGFR-1.

GM-CSF inhibits angiogenesis in mice with HIF-1α-deficient macrophages but not mice with HIF-2α-deficient macrophages

Our model proposes that in HIF-1$\alpha^{flox/flox}$/LysMcre mice, HIF-1α-deficient tumor-infiltrating macrophages would secrete sVEGFR-1 but would secrete reduced amounts of VEGF in response to GM-CSF, resulting in an overall decrease in tumor angiogenesis. Conversely, our model proposes that in HIF-2$\alpha^{flox/+}$/LysMcre mice, VEGF production would be preserved from HIF-2α-deficient tumor-infiltrating macrophages but sVEGFR-1 production would be inhibited, abrogating the anti-angiogenic properties of GM-CSF. In order to determine if the differences in tumor growth that we observed in HIF-1$\alpha^{flox/flox}$/LysMcre and HIF-2$\alpha^{flox/+}$/LysMcre mice were associated with differences in tumor angiogenesis, tumors from each of the mice were stained by immunohistochemistry for the endothelial cell marker CD31. As shown in Figure 2A and 2B, GM-CSF treatment significantly reduced tumor vascularity in both control and HIF-1$\alpha^{flox/flox}$/LysMcre mice ($p = 0.015$ and $p = 0.025$, respectively). Additionally, we observed a decrease in tumor angiogenesis in PBS-treated HIF-1$\alpha^{flox/flox}$/LysMcre mice as compared to PBS-treated control mice, with tumors from GM-CSF-treated HIF-1$\alpha^{flox/flox}$/LysMcre mice showing the lowest amount of vascularity. However, GM-CSF treatment had no effect on tumor vascularity in HIF-2$\alpha^{flox/+}$/LysMcre mice ($p = 0.193$), consistent with the failure of GM-CSF to inhibit tumor growth in these mice.

CD31 immunostaining does not identify functional blood vessels, only endothelial cells present in the tumor, which is insufficient to classify vessels as blood transporters, since many vascular beds within tumors lack lumens and are non-functional. To assess functional blood vessels within the tumors, mice were injected with Texas red-conjugated dextran five minutes prior to sacrifice, and tumors were examined by fluorescent microscopy. Blood flow transports the Texas red-dextran into functional blood vessels, while non-functional vessels remain unlabeled. Consistent with the CD31 immunostaining results, GM-CSF reduced the vascularity of tumors from control mice and HIF-1$\alpha^{flox/flox}$/LysMcre mice ($p = 0.005$ and $p = 0.008$, respectively), but not HIF-2$\alpha^{flox/flox}$/LysMcre mice ($p = 0.576$) (Figure 2C and 2D).

GM-CSF induces VEGF but not sVEGFR-1 in mice with HIF-2α-deficient macrophages

We have shown that macrophage production of VEGF in response to GM-CSF and hypoxia was dependent on HIF-1α, while HIF-2α controlled macrophage production of sVEGFR-1. We next hypothesized that the inability of GM-CSF to inhibit angiogenesis in HIF-2$\alpha^{flox/+}$/LysMcre mice was due to the inability of tumor-infiltrating macrophages in these mice to secrete sVEGFR-1 in response to GM-CSF. We therefore used real-time PCR to evaluate the levels of VEGF and sVEGFR-1 within the tumors of PBS- or GM-CSF-treated mice. Increased levels of sVEGFR-1 were detected within the tumors of GM-CSF-treated LysMcre control mice and HIF-1$\alpha^{flox/flox}$/LysMcre mice ($p = 0.007$ and $p = 0.041$, respectively). However, GM-CSF failed to induce sVEGFR-1 mRNA within the tumors of HIF-2$\alpha^{flox/+}$/LysMcre mice ($p = 0.973$) (Figure 3A). Conversely, GM-CSF increased levels of tumoral VEGF in control and HIF-2$\alpha^{flox/+}$/LysMcre mice ($p = 0.023$ and $p = 0.056$, respectively), but VEGF levels were not elevated within the tumors of HIF-1$\alpha^{flox/flox}$/LysMcre mice treated with GM-CSF ($p = 0.517$) (Figure 3B).

The anti-tumor effects of GM-CSF are dependent on sVEGFR-1 production

We observed increased sVEGFR-1 levels in the tumors of GM-CSF-treated mice, correlating with decreased tumor growth and angiogenesis. To confirm that the modulation

of tumor growth and angiogenesis was due to sVEGFR-1 production, we treated LysMcre control mice or HIF-1α$^{flox/flox}$/LysMcre mice with GM-CSF in the presence or absence of a sVEGFR-1 neutralizing Ab. GM-CSF decreased tumor growth in LysMcre control mice treated with an isotype control antibody ($p = 0.021$), but GM-CSF had no effect on tumor growth in mice treated with the anti-sVEGFR-1 neutralizing Ab ($p = 0.943$) (Figure 4A). GM-CSF also failed to inhibit tumor growth in HIF-1α$^{flox/flox}$/LysMcre mice treated with the sVEGFR-1 neutralizing Ab ($p = 0.627$) (Figure 4B).To confirm the role of sVEGFR-1 production in tumor angiogenesis, we immunostained the tumors from the mice in the sVEGFR-1 neutralization experiment for the endothelial cell marker CD31. As shown in Figure 4C, neutralization of sVEGFR-1 abrogated the anti-angiogenic effects of GM-CSF in both LysMcre and HIF-1α$^{flox/flox}$/LysMcre mice.

Macrophage infiltration of the tumor is preserved in HIF-1α$^{flox/flox}$/LysMcre and HIF-2α$^{flox/+}$/LysMcre mice

We have previously demonstrated that GM-CSF induced macrophage infiltration into murine breast tumors, an effect which correlated with increased sVEGFR-1 production and decreased tumor growth (17). We therefore wanted to determine whether macrophage infiltration into the tumor was altered in HIF-1α$^{flox/flox}$/LysMcre or HIF-2α$^{flox/+}$/LysMcre mice. As shown in Figure 5A and 5B, GM-CSF significantly increased the number of macrophages infiltrating the tumors, as determined by immunostaining for the macrophage marker F4/80 antigen. However, there was no difference in macrophage infiltration in response to GM-CSF between control mice, HIF-1α$^{flox/flox}$/LysMcre mice, or HIF-2α$^{flox/+}$/LysMcre mice. These results demonstrate that ablation of HIF-1α or HIF-2α from the myeloid compartment does not affect macrophage trafficking into the tumor, and indicate that the differences in tumor growth observed in HIF-1α$^{flox/flox}$/LysMcre mice and HIF-2α$^{flox/+}$ mice are due to differences in the phenotype of HIF-1α- and HIF-2α-deficient macrophages, not due to differences in the number of macrophages within the tumor.

GM-CSF inhibits pulmonary metastases in mice with HIF-1α-deficient macrophages

Increased angiogenesis is associated with increased risk of metastasis, both in humans and in murine tumor models. We therefore evaluated lung metastasis following GM-CSF treatment in LysMcre control mice, HIF-1α$^{flox/flox}$/LysMcre mice, and HIF-2α$^{flox/+}$/LysMcre mice. The level of the melanoma-specific gene Pmel17 detected in the lungs was used as an indicator of metastasis (16). Significantly reduced levels of Pmel17 were detected within the lungs of GM-CSF-treated HIF-1α$^{flox/flox}$/LysMcre mice as compared to PBS-treated control mice ($p = 0.047$) (Figure 6, upper panel). However, GM-CSF-treated HIF-2α$^{flox/+}$/LysMcre mice had similar levels of Pmel17 mRNA as PBS-treated controls ($p = 0.822$). Similar results were obtained with real-time PCR for a second melanoma-specific gene, TRP2 (Figure 6, lower panel).

DISCUSSION

GM-CSF has been explored as a cancer therapeutic due to its ability to increase the proliferation and activation of tumor-specific T cells and to enhance antigen presentation from dendritic cells and macrophages. However, intravenous or subcutaneous recombinant GM-CSF was ineffective at limiting melanoma growth in phase I/II studies, and in numerous cases, severe dose-limiting toxicities developed (18, 19). Although systemic therapy with GM-CSF is unsuccessful due to the large pharmacological doses required within the tumor itself, we have previously demonstrated that local, intratumoral injection of GM-CSF is effective at inhibiting tumor growth in a murine cancer model (17). Hurdles for GM-CSF as a therapy for breast cancer include a delivery system that enables high concentrations at the tumor site without the toxic effects of high levels of GM-CSF in the

systemic circulation. We have shown that a major contributor to the anti-tumor effect of GM-CSF is the induction of sVEGFR-1 from tumor macrophages and the removal of free VEGF from bioactivity. Because melanoma is easily accessible for injection, and because tumor-infiltrating macrophages (20, 21) and VEGF (22) each predict poor prognosis in melanoma patients, we chose to investigate the ability of locally administered GM-CSF to inhibit tumor growth, angiogenesis, and metastases in the B16F10 mouse model of melanoma to elucidate the potential for GM-CSF as a novel therapeutic.

We recently published a report demonstrating that macrophage production of VEGF in response to GM-CSF and low O_2 *in vitro* was dependent on HIF-1α, while HIF-2α controlled macrophage production of sVEGFR-1 under the same conditions (10). Here, we extend this study and examine the effect of a myeloid cell-specific deletion of HIF-1α or HIF-2α on the growth of B16F10 melanomas *in vivo*. Taken together, our findings suggest a model in which GM-CSF treatment induces VEGF and sVEGFR-1 from tumor-associated macrophages, resulting in a net inhibition of angiogenesis and a resultant reduction in tumor growth. In mice with HIF-1α-deficient macrophages, GM-CSF induces sVEGFR-1 production but VEGF production is inhibited, resulting in greater decreases in angiogenesis and tumor growth. In mice with HIF-2α-deficient macrophages, GM-CSF fails to induce sVEGFR-1 while VEGF production is preserved, resulting in increased angiogenesis and accelerated tumor growth. Therefore, although hypoxia is canonically considered to be pro-angiogenic, our results demonstrate a significant *anti-angiogenic* effect of hypoxia in a GM-CSF-rich environment. Furthermore, these results demonstrate opposing roles for the HIFs in tumor angiogenesis, with HIF-1α exhibiting pro-angiogenic behavior via its effects on VEGF secretion, in support of Semenza *et al*. (23), and HIF-2α exhibiting anti-angiogenic behavior by inducing the production of the endogenous angiogenesis inhibitor, sVEGFR-1.

Macrophage lysozyme (LysM) is expressed in all cells of the myeloid lineage, including neutrophils as well as monocytes/macrophages. Therefore, HIF-1α or HIF-2α is deleted from neutrophils as well as macrophages in HIF-$1\alpha^{flox/flox}$- or HIF-$2\alpha^{flox/+}$/LysMcre mice. Because neutrophils also express the GM-CSF receptor, it is possible that neutrophils contribute to the sVEGFR-1 production observed in the tumors of GM-CSF-treated mice. In our previous studies, however, neutrophils stimulated with GM-CSF at low O_2 secreted approximately 0.5% of the amount of sVEGFR-1 as an equivalent number of macrophages, an amount which was insufficient to neutralize endogenous VEGF (10). In the current study, we immunostained tumors from PBS- and GM-CSF-treated mice with a neutrophil-specific cell surface marker (clone 7/4, AbD Serotec), and failed to observe an increase in neutrophil migration into the tumor in response to GM-CSF (data not shown). These data suggest that neutrophils do not substantially contribute to sVEGFR-1 production in GM-CSF-treated tumors, indicating that the differences in sVEGFR-1 production, tumor growth, and angiogenesis which we observed are due to ablation of HIF-1α and HIF-2α within the macrophage compartment.

This study utilized HIF-$1\alpha^{flox/flox}$/LysMcre mice, which are homozygous for the floxed HIF-1α allele, and HIF-$2\alpha^{flox/+}$/LysMcre mice, which are heterozygous for the floxed HIF-2α allele. Bone marrow-derived macrophages from these mice contain approximately 50% as much HIF-2α mRNA as macrophages from LysMcre control mice (10). In our previous studies, bone marrow-derived macrophages from HIF-$2\alpha^{flox/+}$/LysMcre mice failed to produce sVEGFR-1 in response to GM-CSF and 0.5% O_2. Furthermore, an approximately 30% knockdown of HIF-2α mRNA by siRNA treatment of bone marrow-derived macrophages from wildtype mice was sufficient to inhibit sVEGFR-1 production (10). It therefore appears that a partial reduction in HIF-2α substantially inhibits sVEGFR-1 production from macrophages stimulated with GM-CSF at hypoxia. Based on these previous findings, we chose to use the HIF-$2\alpha^{flox/+}$/LysMcre mice in the current study even though

HIF-2α was only partially reduced. We observed an approximately 50% increase in tumor growth in mice treated with PBS and the sVEGFR-1 neutralizing antibody as compared to mice treated with PBS and the isotype control (Figures 4A and 4B), suggesting a role for sVEGFR-1 in the growth of the B16F10 tumors, independent of GM-CSF therapy. We had therefore expected that deletion of HIF-2α would decrease endogenous sVEGFR-1 production and increase the rate of tumor growth over that of control mice. However, we observed no difference in tumor growth between HIF-2α$^{flox/+}$/LysMcre mice and LysMcre control mice. We feel that this is likely due to residual sVEGFR-1 production resulting from the partial deletion of HIF-2α, and expect that tumor growth in HIF-2α$^{flox/flox}$/LysMcre mice will be increased as compared to control mice.

The idea of the "angiogenic balance" being shifted toward a pro-angiogenic phenotype by the repression of pro-angiogenic regulators like VEGF has been described by Mazzone *et al*., who showed that PHD2 (the oxygen-dependent regulator of both HIF-1α and VEGF) hemizygosity in mice reduces tumor cell intravasation and metastatic progression in solid tumors, but does not inhibit tumor growth (24). In that study, the loss of VEGF actually acted to repair aberrant and non-functional blood vessels by decreasing vascular leakage. The physiological role of sVEGFR-1 is the regulation of VEGF activity. It might seem that the expression of an "anti-angiogenic" molecule within tissue exposed to hypoxia is counterintuitive, especially when that molecule is up-regulated by a HIF protein. But, unregulated VEGF activity in hypoxic tissue would be counterproductive for the goal of obtaining a fresh blood supply by angiogenesis. VEGF, previously known as VPF or vascular permeability factor, induces vascular leakage, and when in excess (as a result of hypoxia for example), leads to aberrant vessel sprouting and inefficient vasculature. We speculate that the need for a regulator of VEGF activity in a hypoxic environment is essential to maintain this angiogenic balance, and that HIF-2α is the regulator in this process. In this same manner, it is possible that small amounts of sVEGFR-1 production could actually *augment* tumor growth for the same reason – the recuperation of leaky vessels into the tight-junction vascular endothelium required to efficiently deliver blood to the tumors.

This study supports previous findings that macrophages are intimately involved in the metastatic potential of solid tumors (25, 26). Even though, as stated above, deletion of HIF-2α from tumor-associated macrophages did not increase tumor growth, we did observe that the HIF-2α$^{flox/+}$/LysMcre mice had increased pulmonary metastasis compared to the LysMcre control mice. Moreover, in LysMcre control mice, GM-CSF treatment reduced tumor growth but had no effect on pulmonary metastasis, suggesting that macrophage HIF-2α regulates an anti-metastatic pathway, and that the anti-metastatic effect of GM-CSF, previously illustrated in mammary tumors (17), is not observed in this model of malignant melanoma. This data suggest that macrophage HIF-2α alone regulates metastatic genes even in the absence of GM-CSF. Studies to identify these genes are currently underway in our laboratory.

Imtiyaz *et al*. demonstrated that migration of macrophages into hepatocellular carcinoma lesions is inhibited in HIF-2α$^{flox/flox}$/LysMcre mice, an effect that was associated with decreased tumor burden (27). These results suggest that HIF-2α is essential for macrophage recruitment to the tumor microenvironment. The authors characterize the migratory ability of HIF-2α-deficient macrophages *in vitro*, and demonstrate that HIF-2α-deficient macrophages display significantly decreased chemotaxis towards M-CSF, and also express lower levels of the M-CSF receptor and the CXCR4 receptor (27). However, we observed no difference in the number of tumor-infiltrating macrophages in B16F10 melanomas in PBS-treated control mice, HIF-1α$^{flox/flox}$/LysMcre mice, or HIF-2α$^{flox/+}$/LysMcre mice. Furthermore, GM-CSF treatment increased macrophage infiltration of the tumor

equivalently in mice of each genotype, suggesting that neither HIF-1α nor HIF-2α deletion had an effect on GM-CSF-induced macrophage chemotaxis in this model. Macrophage infiltration of different tumors is likely due to the expression of different chemotactic factors. For example, GM-CSF induces overexpression of macrophage chemoattractant CCL2 in mammary breast tumors (28). Further studies are ongoing in our lab to characterize the stimuli that drive macrophage infiltration of B16F10 melanoma tumors, as well as to determine the extent to which HIF-1α and HIF-2α regulate macrophage chemotaxis in response to these factors.

We have shown that GM-CSF is effective at limiting tumor growth and angiogenesis in mammary tumors and now in a mouse model of malignant melanoma, but that it is only effective when delivered intratumorally at pharmacological doses. Intravenous GM-CSF has been explored as a melanoma treatment due to its effects on the proliferation and activation of T cells, but was ineffective as a cancer therapeutic when delivered systemically, and in many cases, severe dose-limiting toxicities developed. The use of GM-CSF delivered intratumorally avoids this toxicity and can be easily administered to melanoma patients in the clinical setting.

REFERENCES

1. Steele RJ, Brown M, Eremin O. Characterisation of macrophages infiltrating human mammary carcinomas. Br. J. Cancer. 1985; 51:135–138. [PubMed: 3155620]
2. Lissbrant IF, Stattin P, Wikstrom P, Damber JE, Egevad L, Bergh A. Tumor associated macrophages in human prostate cancer: relation to clinicopathological variables and survival. Int. J. Oncol. 2000; 17:445–451. [PubMed: 10938382]
3. Bingle L, Brown NJ, Lewis CE. The role of tumour-associated macrophages in tumour progression: implications for new anticancer therapies. J. Pathol. 2002; 196:254–265. [PubMed: 11857487]
4. Leek RD, Hunt NC, Landers RJ, Lewis CE, Royds JA, Harris AL. Macrophage infiltration is associated with VEGF and EGFR expression in breast cancer. J. Pathol. 2000; 190:430–436. [PubMed: 10699991]
5. Lewis JS, Landers RJ, Underwood JC, Harris AL, Lewis CE. Expression of vascular endothelial growth factor by macrophages is up-regulated in poorly vascularized areas of breast carcinomas. J. Pathol. 2000; 192:150–158. [PubMed: 11004690]
6. Manalo DJ, Rowan A, Lavoie T, Natarajan L, Kelly BD, Ye SQ, Garcia JG, Semenza GL. Transcriptional regulation of vascular endothelial cell responses to hypoxia by HIF-1. Blood. 2005; 105:659–669. [PubMed: 15374877]
7. Eubank TD, Roberts R, Galloway M, Wang Y, Cohn DE, Marsh CB. GM-CSF induces expression of soluble VEGF receptor-1 from human monocytes and inhibits angiogenesis in mice. Immunity. 2004; 21:831–842. [PubMed: 15589171]
8. Kendall RL, Thomas KA. Inhibition of vascular endothelial cell growth factor activity by an endogenously encoded soluble receptor. Proc. Natl. Acad. Sci. U. S. A. 1993; 90:10705–10709. [PubMed: 8248162]
9. Kendall RL, Wang G, Thomas KA. Identification of a natural soluble form of the vascular endothelial growth factor receptor, FLT-1, and its heterodimerization with KDR. Biochem. Biophys. Res. Commun. 1996; 226:324–328. [PubMed: 8806634]
10. Eubank TD, Roda JM, Liu H, O'Neil T, Marsh CB. Opposing roles for HIF-1{alpha} and HIF-2{alpha} in the regulation of angiogenesis by mononuclear phagocytes. Blood. 2010
11. Leek RD, Talks KL, Pezzella F, Turley H, Campo L, Brown NS, Bicknell R, Taylor M, Gatter KC, Harris AL. Relation of hypoxia-inducible factor-2 alpha (HIF-2 alpha) expression in tumor-infiltrative macrophages to tumor angiogenesis and the oxidative thymidine phosphorylase pathway in Human breast cancer. Cancer Res. 2002; 62:1326–1329. [PubMed: 11888900]
12. Talks KL, Turley H, Gatter KC, Maxwell PH, Pugh CW, Ratcliffe PJ, Harris AL. The expression and distribution of the hypoxia-inducible factors HIF-1alpha and HIF-2alpha in normal human

tissues, cancers, and tumor-associated macrophages. Am. J. Pathol. 2000; 157:411–421. [PubMed: 10934146]

13. Cramer T, Yamanishi Y, Clausen BE, Forster I, Pawlinski R, Mackman N, Haase VH, Jaenisch R, Corr M, Nizet V, Firestein GS, Gerber HP, Ferrara N, Johnson RS. HIF-1alpha is essential for myeloid cell-mediated inflammation. Cell. 2003; 112:645–657. [PubMed: 12628185]
14. Skuli N, Liu L, Runge A, Wang T, Yuan L, Patel S, Iruela-Arispe L, Simon MC, Keith B. Endothelial deletion of hypoxia-inducible factor-2alpha (HIF-2alpha) alters vascular function and tumor angiogenesis. Blood. 2009; 114:469–477. [PubMed: 19439736]
15. Clausen BE, Burkhardt C, Reith W, Renkawitz R, Forster I. Conditional gene targeting in macrophages and granulocytes using LysMcre mice. Transgenic Res. 1999; 8:265–277. [PubMed: 10621974]
16. Tsukamoto K, Hirata S, Osada A, Kitamura R, Shimada S. Detection of circulating melanoma cells by RT-PCR amplification of three different melanocyte-specific mRNAs in a mouse model. Pigment Cell Res. 2000; 13:185–189. [PubMed: 10885678]
17. Eubank TD, Roberts RD, Khan M, Curry JM, Nuovo GJ, Kuppusamy P, Marsh CB. Granulocyte macrophage colony-stimulating factor inhibits breast cancer growth and metastasis by invoking an anti-angiogenic program in tumor-educated macrophages. Cancer Res. 2009; 69:2133–2140. [PubMed: 19223554]
18. Locke F, Clark JI, Gajewski TF. A phase II study of oxaliplatin, docetaxel, and GM-CSF in patients with previously treated advanced melanoma. Cancer Chemother. Pharmacol. 2010; 65:509–514. [PubMed: 19597729]
19. Ravaud A, Delaunay M, Chevreau C, Coulon V, Debled M, Bret-Dibat C, Courbon F, Gualde N, Nguyen Bui B. Granulocyte-macrophage colony-stimulating factor alone or with dacarbazine in metastatic melanoma: a randomized phase II trial. Br. J. Cancer. 2001; 85:1467–1471. [PubMed: 11720430]
20. Shi L, Lei D, Ma C, Xu F, Li Y, Wang Y, Cong N, Liu D, Pan XL. Clinicopathological implications of tumour-associated macrophages and vascularization in sinonasal melanoma. J. Int. Med. Res. 2010; 38:1276–1286. [PubMed: 20926000]
21. Ly LV, Baghat A, Versluis M, Jordanova ES, Luyten GP, van Rooijen N, van Hall T, van der Velden PA, Jager MJ. In aged mice, outgrowth of intraocular melanoma depends on proangiogenic M2-type macrophages. J. Immunol. 2010; 185:3481–3488. [PubMed: 20713886]
22. Ascierto PA, Leonardi E, Ottaiano A, Napolitano M, Scala S, Castello G. Prognostic value of serum VEGF in melanoma patients: a pilot study. Anticancer Res. 2004; 24:4255–4258. [PubMed: 15736481]
23. Semenza GL. Vasculogenesis, angiogenesis, and arteriogenesis: mechanisms of blood vessel formation and remodeling. J. Cell. Biochem. 2007; 102:840–847. [PubMed: 17891779]
24. Mazzone M, Dettori D, Leite de Oliveira R, Loges S, Schmidt T, Jonckx B, Tian YM, Lanahan AA, Pollard P, Ruiz de Almodovar C, De Smet F, Vinckier S, Aragones J, Debackere K, Luttun A, Wyns S, Jordan B, Pisacane A, Gallez B, Lampugnani MG, Dejana E, Simons M, Ratcliffe P, Maxwell P, Carmeliet P. Heterozygous deficiency of PHD2 restores tumor oxygenation and inhibits metastasis via endothelial normalization. Cell. 2009; 136:839–851. [PubMed: 19217150]
25. Hiraoka K, Zenmyo M, Watari K, Iguchi H, Fotovati A, Kimura YN, Hosoi F, Shoda T, Nagata K, Osada H, Ono M, Kuwano M. Inhibition of bone and muscle metastases of lung cancer cells by a decrease in the number of monocytes/macrophages. Cancer. Sci. 2008; 99:1595–1602. [PubMed: 18754872]
26. Lin EY, Nguyen AV, Russell RG, Pollard JW. Colony-stimulating factor 1 promotes progression of mammary tumors to malignancy. J. Exp. Med. 2001; 193:727–740. [PubMed: 11257139]
27. Imtiyaz HZ, Williams EP, Hickey MM, Patel SA, Durham AC, Yuan LJ, Hammond R, Gimotty PA, Keith B, Simon MC. Hypoxia-inducible factor 2alpha regulates macrophage function in mouse models of acute and tumor inflammation. J. Clin. Invest. 2010; 120:2699–2714. [PubMed: 20644254]
28. Owen JL, Torroella-Kouri M, Handel-Fernandez ME, Iragavarapu-Charyulu V. GM-CSF up-regulates the expression of CCL2 by T lymphocytes in mammary tumor-bearing mice. Int. J. Mol. Med. 2007; 20:129–136. [PubMed: 17549399]

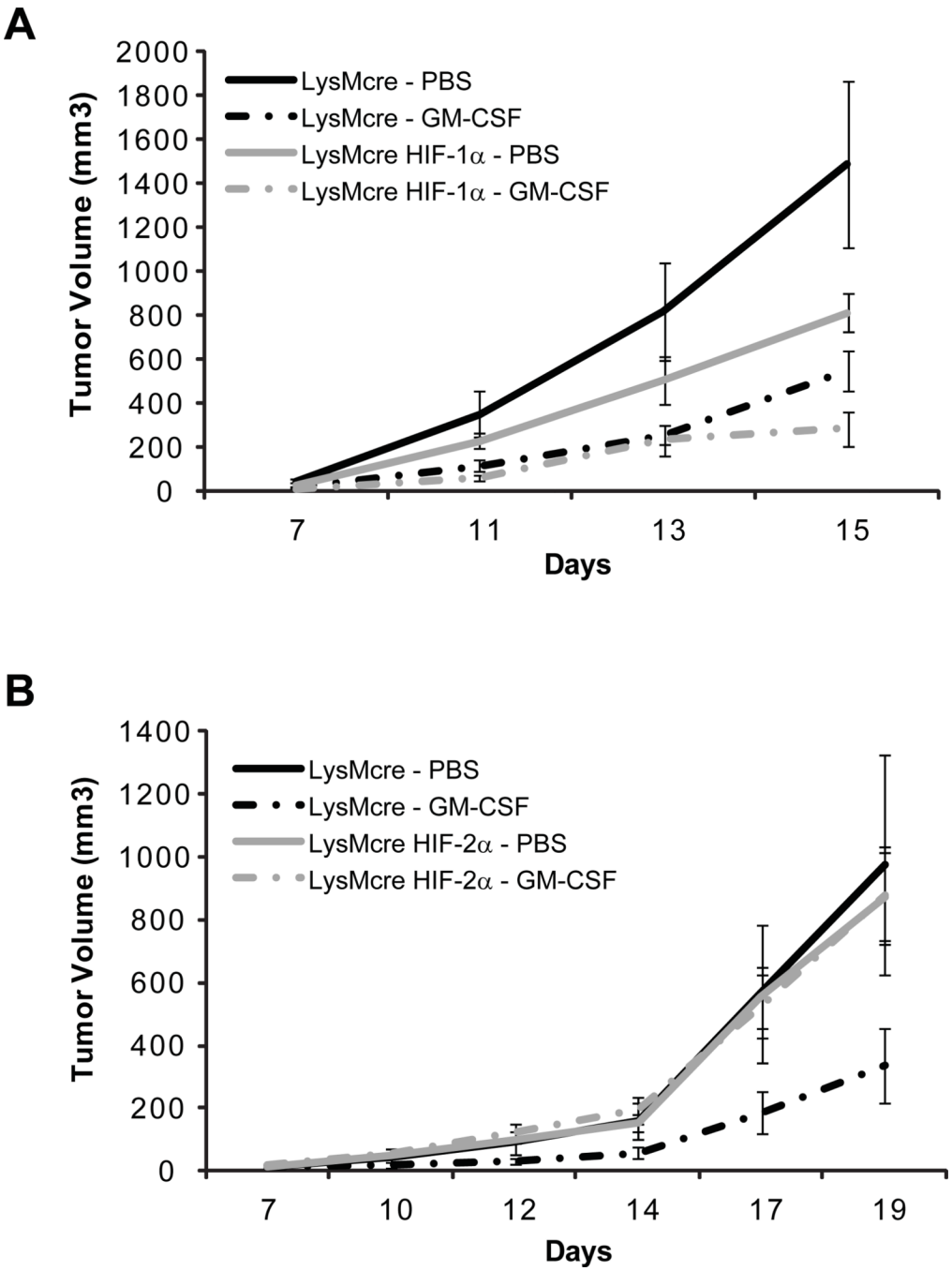

Figure 1. GM-CSF fails to inhibit tumor growth in mice with HIF-2α-deficient macrophages

(A) HIF-1α$^{flox/fox}$/LysMcre mice are homozygous for a floxed HIF-1α allele and for cre recombinase driven from a myeloid-specific promoter, LysMcre. LysMcre control mice contain the LysM-driven cre recombinase but no floxed alleles. Control mice or HIF-1α$^{flox/fox}$/LysMcre mice with subcutaneous B16F10 tumors were treated intratumorally 3×/week with PBS or murine GM-CSF. Tumor dimensions were measured 3×/week, and tumor volumes were calculated as described in the Methods section. (B) HIF-2α$^{flox/+}$ mice are heterozygous for a floxed HIF-2α allele and homozygous for LysM-driven cre recombinase. These mice contain approximately 50% the levels of HIF-2α mRNA as control mice, but bone marrow-derived macrophages from these mice do not secrete sVEGFR-1 in

response to GM-CSF (10). HIF-2α$^{flox/+}$ mice or LysMcre control mice bearing B16F10 melanomas were treated with PBS or GM-CSF and tumor volumes were calculated as described in (A). For both A and B, each data point represents the mean tumor volume ± SEM of at least 15 mice per group.

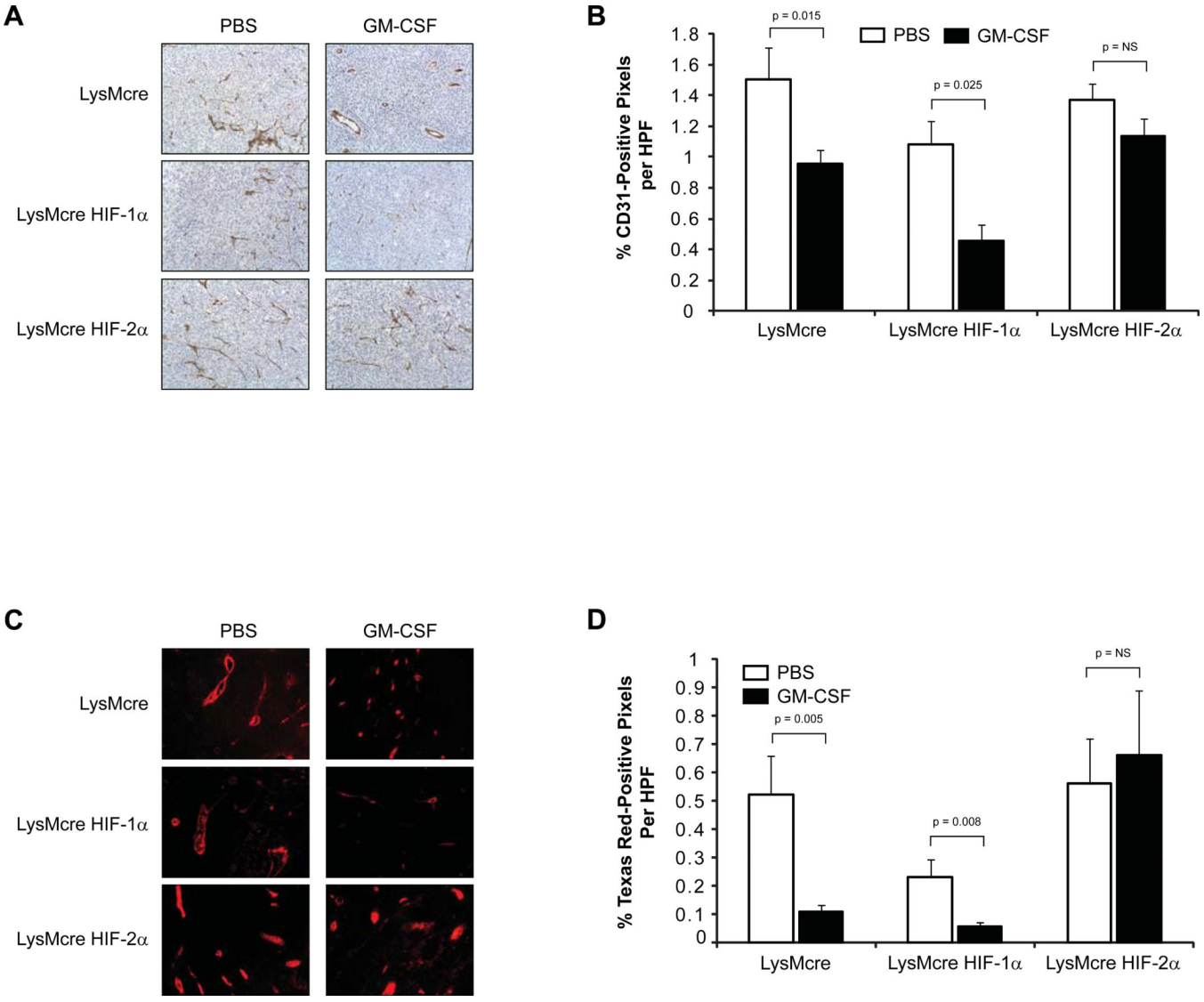

Figure 2. GM-CSF fails to inhibit angiogenesis in mice with HIF-2α-deficient macrophages

HIF-1α$^{flox/flox}$/LysMcre mice, HIF-2α$^{flox/+}$/LysMcre mice, and LysMcre control mice were treated with PBS or GM-CSF, as described in Figure 1. At the time of sacrifice, tumors were harvested, fixed in 10% formalin, and stained for CD31 by immunohistochemistry. (A) Representative images from mice in each of the treatment groups. (B) CD31 immunostaining was digitally quantified by comparing the number of CD31-positive pixels to the total number of pixels in each high-powered field (HPF) for stitched images taken across entire tumors. The graph shows the average percentage of CD31-positive pixels for at least 15 mice per treatment group. (C) Mice from the experiment described in Figure 1 were injected with a fluorescently labeled dextran immediately prior to sacrifice. Tumors were harvested and sections were imaged with a fluorescent microscope to assess the extent of functional blood vessel development within the tumor. Representative samples from tumors taken from each group are shown. (D) Stitched images taken across the entire tumor of each mouse were digitally quantified for the number of fluorescent pixels. The graph shows the average percentage of Texas red-positive pixels for at least 10 mice per treatment group.

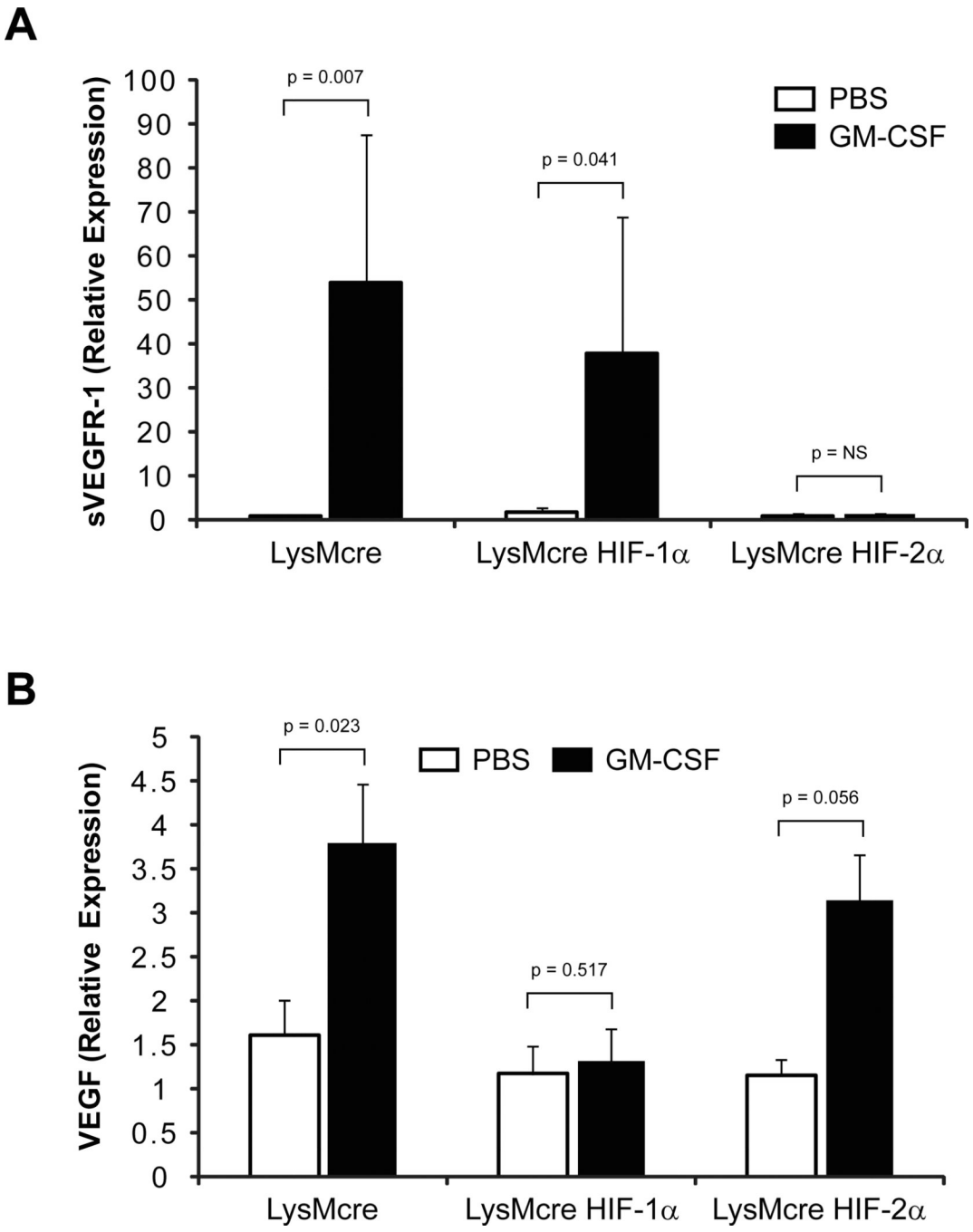

Figure 3. GM-CSF fails to induce intratumoral sVEGFR-1 in mice with HIF-2α-deficient macrophages

Mice with HIF-1α -or HIF-2α-deficient macrophages were treated with PBS or GM-CSF, as shown in Figure 1. At the time of sacrifice, tumor sections were excised and flash-frozen in liquid nitrogen. Frozen tissue was pulverized in liquid nitrogen and dissolved in TRIzol. Real-time PCR was performed for sVEGFR-1 (A) or VEGF (B). Results represent the mean ± SEM mRNA level as compared to the levels in PBS-treated control mice. Each group contains at least 15 mice.

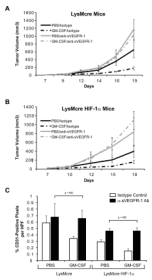

Figure 4. The inhibition of tumor growth and angiogenesis by GM-CSF is dependent on sVEGFR-1 production

LysMcre control mice (A) or HIF-1α$^{flox/flox}$/LysMcre mice (B) were treated 3×/week with PBS or GM-CSF, and an isotype control antibody or an anti-sVEGFR-1 neutralizing antibody. Tumor dimensions were measured and tumor volumes were calculated as described in Figure 1. For both A and B, each data point represents the mean tumor volume ± SEM of at least 10 mice per group. (C) At the time of sacrifice, tumors from mice in Figure 4A and 4B were fixed in 10% formalin and labeled for CD31 by immunohistochemistry. CD31 staining was quantified as described in Figure 2.

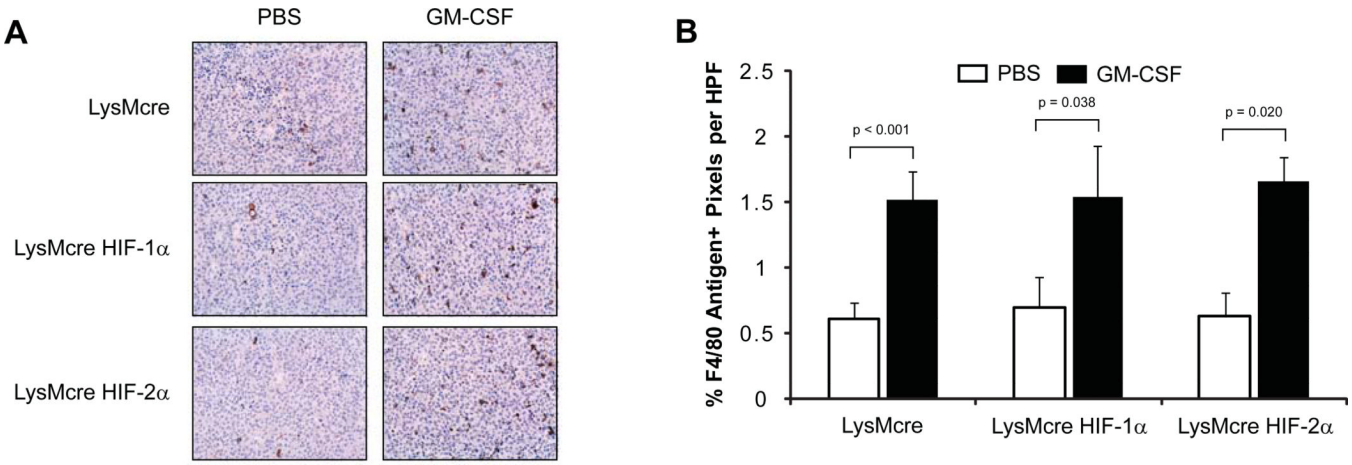

Figure 5. Macrophage infiltration of tumors in response to GM-CSF is unaffected by deletion of HIF-1α or HIF-2α

HIF-1α$^{flox/flox}$/LysMcre mice, HIF-2α$^{flox/+}$/LysMcre mice, and LysMcre control mice were treated with PBS or GM-CSF, as described in Figure 1. At the time of sacrifice, tumors were harvested, fixed in 10% formalin, and stained for the murine macrophage marker F4/80 antigen by immunohistochemistry. (A) Representative images from mice in each of the treatment groups. (B) F4/80 antigen immunostaining was digitally quantified by comparing the number of positive (brown) pixels to the total number of pixels in each high-powered field (HPF) for stitched images taken across entire tumors. The graph shows the average percentage of F4/80 antigen-positive pixels for at least 10 mice per treatment group.

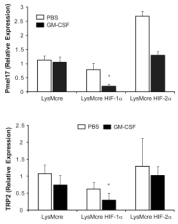

Figure 6. GM-CSF inhibits pulmonary metastases in mice with HIF-1α-deficient macrophages

Mice with HIF-1α -or HIF-2α-deficient macrophages were treated with PBS or GM-CSF, as shown in Figure 1. At the time of sacrifice, lungs were flash-frozen in liquid nitrogen. Frozen tissue was pulverized in liquid nitrogen and dissolved in TRIzol to extract RNA. A nested real-time PCR was performed for the melanoma-specific proteins Pmel17 (top panel) and TRP2 (bottom panel). Results represent the mean ± SEM mRNA level in each treatment group as compared to the levels in PBS-treated control mice. Each group contains at least 10 mice. *, $p < 0.05$ vs. PBS-treated LysMcre control mice.